Published online 27 May 2017

Nucleic Acids Research, 2017, Vol. 45, No. 12 ***7367–7381***
doi: 10.1093/nar/gkx487

Self-protective responses to norvaline-induced stress in a leucyl-tRNA synthetase editing-deficient yeast strain

Quan-Quan Ji[1,†], Zhi-Peng Fang[1,†], Qing Ye[1], Cheng-Wu Chi[1] and En-Duo Wang[1,2,*]

[1]State Key Laboratory of Molecular Biology, CAS Center for Excellence in Molecular Cell Science, Shanghai Institute of Biochemistry and Cell Biology, Chinese Academy of Sciences; University of Chinese Academy of Sciences, 320 Yueyang Road, Shanghai 200031, P. R. China and [2]School of Life Science and Technology, Shanghai Tech University, 100 Haike Road, Shanghai 201210, P. R. China

Received December 02, 2016; Revised May 18, 2017; Editorial Decision May 20, 2017; Accepted May 24, 2017

ABSTRACT

The editing function of aminoacyl-tRNA synthetases (aaRSs) is indispensible for formation of the correct aminoacyl-tRNAs. Editing deficiency may lead to growth inhibition and the pathogenesis of various diseases. Herein, we confirmed that norvaline (Nva) but not isoleucine or valine is the major threat to the editing function of *Saccharomyces cerevisiae* leucyl-tRNA synthetase (*Sc*LeuRS), both *in vitro* and *in vivo*. Nva could be misincorporated into the proteome of the LeuRS editing-deficient yeast strain (D419A/*Sc*Δ*leuS*), potentially resulting in dysfunctional protein folding and growth delay. Furthermore, the exploration of the Nva-induced intracellular stress response mechanism in D419A/*Sc*Δ*leuS* revealed that Hsp70 chaperones were markedly upregulated in response to the potential protein misfolding. Additionally, proline (Pro), glutamate (Glu) and glutamine (Gln), which may accumulate due to the conversion of Nva, collectively contributed to the reduction of reactive oxygen species (ROS) levels in Nva-treated D419A/*Sc*Δ*leuS* cells. In conclusion, our study highlights the significance of the editing function of LeuRS and provides clues for understanding the intracellular stress protective mechanisms that are triggered in aaRS editing-deficient organisms.

INTRODUCTION

Aminoacyl-tRNA synthetases (aaRSs) are responsible for charging their cognate tRNAs with the corresponding amino acids to generate aminoacyl-tRNAs for protein biosynthesis (1). For most aaRSs, the aminoacylation reaction occurs in two steps: amino acid activation and tRNA aminoacylation. In more detail, aaRSs use adenosine triphosphate (ATP) to activate amino acid by generating aminoacyl-adenylate (aa-AMP) intermediates, and the aminoacyl moiety is then transferred to the tRNA to form aminoacyl-tRNA (aa-tRNA) (1,2). Since many amino acids and some of their metabolic intermediates share similar structures, there is the potential for a specific aaRS to mischarge non-cognate amino acids; and to counteract this and ensure translation fidelity, many aaRSs use a 'double-sieve' mechanism to eliminate non-cognate amino acids (3,4). The first sieve involves the catalytic active site, which can discriminate different amino acids. For many closely related or slightly smaller amino acids, some aaRSs have evolved a distinct editing active site that acts as a second sieve to hydrolyze misactivated or mischarged amino acids (3,5).

Based on the sequence and architecture of the catalytic domain, aaRSs are divided into two classes (6,7). Leucyl-tRNA synthetase (LeuRS), as well as isoleucyl-tRNA synthetase (IleRS) and valyl-tRNA synthetase (ValRS), belongs to class I aaRSs that share a common Rossmann fold and two conserved HIGH and KMSKS motifs in their catalytic domains (6,8–11). Besides the cognate Leu, LeuRS can also activate norvaline (Nva), isoleucine (Ile) and valine (Val) (12–15). The non-proteinogenic Nva is a metabolic side product of leucine (Leu) biosynthesis and it differs from Leu only by a single methyl group, posing a prime threat to the fidelity of leucylation (16). Under microaerobic conditions, Nva can accumulate in *Escherichia coli* and be misincorporated into the proteome to the extent that ∼10% of Leu residues are substituted with Nva (17,18). Nva can also be misincorporated into antibacterial peptides produced by *Bacillus subtilis* and recombinant human haemoglobin produced in *E. coli* cells under certain conditions (19,20). To prevent non-cognate amino acids from being misincorporated into newly synthesized proteins, LeuRS performs both pre-transfer (hydrolysis of aa-AMP) and post-transfer (hydrolysis of aa-tRNA) editing to

*To whom correspondence should be addressed. Tel: +86 21 5492 1241; Fax: +86 21 5492 1011; Email: edwang@sibs.ac.cn
†These authors contributed equally to the paper as first authors.

ensure translation accuracy (5,21–24). For *Saccharomyces cerevisiae* LeuRS (*Sc*LeuRS), post-transfer editing is an important proofreading mechanism that preserves yeast cell survival in the presence of surplus Nva *in vivo* (25). The connective peptide 1 (CP1), which is flexibly inserted into the catalytic domain, performs post-transfer editing (12,22,26–28). In particular, a conserved Asp within the CP1 domain of LeuRS (*Ec*LeuRS-Asp^{345}, *Natrialba magadii* LeuRS1-Asp^{354}, *Sc*LeuRS-Asp^{419} and *Homo sapiens* LeuRS-Asp^{399}) is responsible for the post-transfer editing activity, and mutation of this Asp to Ala could completely abolish this activity (24,25,29,30).

A deficiency in aaRS editing activity may lead to proteomic instability, cell growth inhibition and severe disruption of physiological function (31–34). For example, editing deficiency of alanyl-tRNA synthetase induces neurodegeneration and cardiac proteinopathy in mice (31,32). In aging bacteria with an editing-defective IleRS, the SOS response mechanism was activated and the DNA mutation rate was dramatically increased (33). A recent study found that Nva but not Ile was the biggest threat to the fidelity of LeuRS activity in editing-defective *E.coli*, emphasizing the importance of LeuRS editing in ensuring the survival of bacteria in environments with fluctuating oxygen levels (16). However, the detailed stress protective mechanism induced by non-cognate substrates in editing-deficient organisms is little understood. Herein, we utilized a LeuRS post-transfer editing-deficient yeast strain (D419A/*Sc*Δ*leuS*) to address this question.

The heat shock response is the most universal stress adaptation mechanism in organisms, involving the upregulation of heat shock proteins (Hsp) that facilitate refolding or degradation of misfolded proteins and prevent their aggregation (35). In *Saccharomyces cerevsiae*, there are eight Hsp70 family members, of which six are localized in the cytoplasm or nucleus (SSA1, SSA2, SSA3, SSA4, SSB1 and SSB2) and two (KAR2 and SSC) are localized in organelles (35). KAR2, also known as Bip, is the sole Hsp70 chaperone in the endoplasmic reticulum (ER), whose upregulation can relieve ER stress (35,36). Besides, there are two Hsp90 homologs (Hsc82 and Hsp82) in *S. cerevsiae* that are responsible for quality control of mature proteins and macromolecular assemblies (35).

In addition to the heat shock response, organisms could accumulate specific small molecules to counteract stress. Proline (Pro) is a well-known multifunctional stress protectant which inhibits protein aggregation and scavenges intracellular reactive oxygen species (ROS) (37–39). Pro content increases under certain stress conditions in plants (40), and yeasts that accumulate Pro are more tolerant to stress (37). Pro can be synthesized from glutamate (Glu) stepwise by glutamate kinase (Pro1), γ-glutamyl phosphate reductase (Pro2) and P5C reductase (Pro3) (41). Additionally, in *S. cerevsiae* cells, arginine (Arg) can be converted to ornithine (Orn) by arginase (CAR1), and Orn is then converted to Pro by ornithine transaminase (CAR2) (42,43). Pro can be converted back to Glu in mitochondria by Pro dehydrogenase (PUT1) and P5C dehydrogenase (PUT2) (44,45). Glu can be converted to glutamine (Gln), and *vice versa*. The riboflavin transporter (MCH5) is a plasma membrane-bound protein that transports riboflavin into the cytosol and produces flavin adenine dinucleotide (FAD) which serves as the cofactor for PUT1 (46). Importantly, Pro, Glu and Gln are all *bona fide* ROS scavengers. Pro can quench ·OH and O_2^- radicals due to its low ionization potential (38). Gln can be used to generate Glu and maintain an appropriate intracellular Glu pool, and then Glu can be used directly for the synthesis of glutathione, which is a major redox buffering compound (47). In addition, Glu and Gln can be converted to α-ketoglutarate (α-KG), which then enter the TCA cycle to supply NADPH and ATP-producing pathways (48).

In this study, we confirmed that Nva is the major editing target of *Sc*LeuRS and can significantly inhibit the growth of the *Sc*Δ*leuS* strain harboring the editing-deficient *Sc*LeuRS-D419A (D419A/*Sc*Δ*leuS*). Nva can be misincorporated into the proteome of D419A/*Sc*Δ*leuS*, which may cause protein instability and the upregulation of heat shock proteins. To reduce the cytotoxicity of Nva, D419A/*Sc*Δ*leuS* cells may initiate protective responses to convert some Nva to non-toxic metabolites, such as Pro, Glu and Gln. The accumulation of these antioxidative amino acids can lead to the reduction of intracellular ROS levels. In conclusion, our results provide a better understanding of the intracellular protective mechanisms in response to aaRS editing deficiency induced stress and provided insights into aaRS editing deficiency associated diseases.

MATERIALS AND METHODS

Materials

L-Leu, L-Nva, BioUltra L-Ile, BioUltra L-Val, dithiothreitol (DTT), ATP, CTP, GTP, UTP, 5′-GMP, tetrasodium pyrophosphate, inorganic pyrophosphate, Tris–HCl, $MgCl_2$, NaCl and activated charcoal were purchased from Sigma-Aldrich (St Louis, MO, USA). Pyrophosphatase (PPiase) was obtained from Roche Applied Science (Switzerland). [^{3}H]Leu, [^{32}P]tetrasodium pyrophosphate and [α-^{32}P]ATP were obtained from PerkinElmer Inc. (Waltham, MA, USA). Nuclease S1 was obtained from Thermo Scientific (Pittsburgh, PA, USA). Ni^{2+}-NTA Superflow resin was purchased from Qiagen Inc. (Germany). Amicon Ultra 15 ml centrifugal concentrators (cutoff 30 kDa), Amicon Ultra 4 ml centrifugal concentrators (cutoff 3 kDa), polyethyleneimine cellulose plates and nitrocellulose membranes (0.22 μm) were purchased from Merck (Germany). Minimal SD medium, YPD medium and the Yeastmaker Yeast Transformation System 2 was purchased from Clontech (Japan). SYBR Green Real-time PCR Master Mix was purchased from Toyobo (Japan). Primescript RT Master Mix was obtained from Takara (Japan). An AccQ-Fluor reagent kit was purchased from Waters (Milford, MA, USA). The dNTP mixture was obtained from Sangon (China). A ROS assay kit was obtained from Beyotime Biotechnology (China). A plasmid extraction kit and DNA fragment rapid purification kit were purchased from Tiangen (China). Oligonucleotide primers were synthesized by Biosune Bioscience (China). Competent *E. coli* Top10 and Rosetta 2 (DE3) cells were prepared in our laboratory.

Gene cloning, expression and protein purification

Recombinant plasmids pET28a-*Sc*LeuRS and pET28a-*Sc*LeuRS-D419A were constructed in our laboratory (25) and transformed into *E. coli* Rosetta 2 (DE3) cells for protein expression. Purified proteins were dialysed into buffer A (20 mM Tris–HCl pH 8.0, 100 mM NaCl) in an Amicon Ultra 15 ml centrifugal concentrator (cutoff 30 kDa), concentrated to ∼300 μl, and mixed gently with the same volume of glycerol and stored at −20°C.

Gene transcription and [^{32}P]-labeling of tRNA

A plasmid containing the T7 promoter sequence and *Ca*tRNA^{Leu}(UAA) gene was constructed in our previous work (49). Forward (5'-ctaatacgactcactataggag-3') and reverse (5'-tggtgaagggtgcgagattcg-3') primers were used to polymerase chain reaction (PCR)-amplify the DNA template for *in vitro* transcription. Transcription, purification and [^{32}P]-labeling of *Ca*tRNA^{Leu}(UAA) were performed according to our previously reported method (49).

ATP-PPi exchange

The amino acid activation activity of *Sc*LeuRS for different amino acids was measured in reactions containing 60 mM Tris–HCl (pH 7.5), 10 mM $MgCl_2$, 2 mM DTT, 4 mM ATP, 2 mM [^{32}P]tetrasodium pyrophosphate (22 CPM/mol) and 10–1000 μM Leu, 0.3–30 mM Nva, 5–100 mM Ile or 3–150 mM Val. Reactions were started by the addition of 50–100 nM *Sc*LeuRS after incubation at 30°C for 2–3 min. Aliquots (9 μl) at specific time points were added to 200 μl of quenching solution (2% activated charcoal, 3.5% $HClO_4$ and 50 mM tetrasodium pyrophosphate).Whatman GF/C filter papers were used to collect the activated charcoal after it had sufficiently absorbed the generated [^{32}P]ATP following vortexing. Radioactivity was then measured by liquid scintillation counting.

Aminoacylation and deacylation

In previous studies, yeast total tRNA was widely used to measure the aminoacylation and editing activities of *Sc*LeuRS, because both *in vitro* transcribed *S. cerevisiae* tRNA^{Leu} (*Sc*tRNA^{Leu}) and *Sc*tRNA^{Leu} overexpressed in *E. coli* possess negligible accepting activity (50). However, yeast total tRNA still showed low activity as a mixture. We previously reported that the transcribed *Candida albicans* tRNA^{Leu}(UAA) [*Ca*tRNA^{Leu}(UAA)] is well recognized by *Sc*LeuRS (49). Therefore, we used transcribed *Ca*tRNA^{Leu}(UAA) to assay the misaminoacylation and editing activities of *Sc*LeuRS.

Aminoacylation reactions contained 60 mM Tris–HCl (pH 7.5), 10 mM $MgCl_2$, 2 mM DTT, 4 mM ATP, variable concentrations of *Ca*tRNA^{Leu}, [^{32}P]*Ca*tRNA^{Leu}, different amino acids (Leu/Nva/Ile/Val) and 200 nM *Sc*LeuRS or *Sc*LeuRS-D419A. Aliquots (9 μl) were removed at specific time points for ethanol precipitation with NaAc (pH 5.2) at −20 °C overnight. Precipitated samples were centrifuged at 12 000 × *g* at 4°C for 30 min, dried at room temperature for 30 min and digested with 6 μl of nuclease S1 (25 U) for 1 h at 37°C. Thin-layer chromatography (TLC) was performed in 0.1 M NH_4Ac and 5% acetic acid. After visualization by phosphorimaging, the results were analyzed using Multi-Gauge Version 3.0 software (FUJIFILM).

Leu-[^{32}P]*Ca*tRNA^{Leu}, Nva-[^{32}P]*Ca*tRNA^{Leu}, Ile-[^{32}P]*Ca*tRNA^{Leu} and Val-[^{32}P]*Ca*tRNA^{Leu} were prepared by the reaction of *Sc*LeuRS-D419A and subsequent phenol (pH 4.5)/chloroform extraction and ethanol precipitation. The deacylation reaction was performed in 60 mM Tris–HCl (pH 7.5), 10 mM $MgCl_2$ and 100–500 nM *Sc*LeuRS or *Sc*LeuRS-D419A at 30°C. Reactions were started by the addition of 3.5 μM crude aminoacylated tRNA^{Leu}. Samples were treated in the same way as described above for the aminoacylation reaction.

Construction of WT/*Sc*Δ*leuS* and D419A/*Sc*Δ*leuS* strains

The yeast knockout strain *Sc*Δ*leuS* that contains the rescue plasmid p416GPD-*Sc*LeuRS was constructed in our lab previously (51). The gene encoding *Sc*LeuRS was subcloned from pET28a-*Sc*LeuRS-6 × His and inserted into the PstI and XhoI restriction enzyme sites of p425TEF to generate p425TEF-*Sc*LeuRS-6 × His. p425TEF-*Sc*LeuRS-D419A-6 × His was obtained by site-directed mutagenesis using p425TEF-*Sc*LeuRS-6 × His as a template. The *Sc*Δ*leuS* strain was cultured in yeast extract peptone dextrose adenine (YPDA) medium overnight at 30°C, and plasmids were respectively transformed into *Sc*Δ*leuS* using the Yeastmaker Yeast Transformation System 2 according to the manufacture's protocol. Transformants were cultured on SD/Leu$^-$/5-FOA plates to discard the rescue plasmid, and surviving transformants were picked and named WT/*Sc*Δ*leuS* and D419A/*Sc*Δ*leuS*, respectively (Figure 2A).

Yeast total RNA extraction and transcriptional profile analysis

Yeast cells (WT/*Sc*Δ*leuS* and D419A/*Sc*Δ*leuS*) were cultured in 50 ml SD/Leu$^-$ medium for 12 h to A_{600} = 0.6. Each strain was then supplemented with or without 0.5 mM Nva and culturing for 12 h. Total RNA from WT/*Sc*Δ*leuS* and D419A/*Sc*Δ*leuS* was extracted using the hot phenol method according to previous reports (52). Yeast cells were suspended in 400 μl AE buffer (50 mM NaAc pH5.2, 10 mM ethylenediaminetetraacetic acid (EDTA)). A total of 40 μl 10% sodium dodecyl sulphate and 400 μl acidic saturated phenol (pH 4.5) were then added and vortexed for 5–10 s. Samples were incubated at 65°C for 10 min to ensure sufficient lysis and vortexed for 5–10 s per min. Samples were then incubated on ice for 5 min, centrifuged at 15 000 × *g* for 10 min at 4°C and supernatants were extracted with an equivalent volume of phenol (pH 4.5) and chloroform/isoamylol (24:1) in order. Samples were then mixed with 1 ml ethanol and 40 μl 3 M NaAc (pH 5.2) for precipitation. Precipitated total RNA was centrifuged, dried and resolved in 50 μl ddH_2O. After quality verification, total RNA was sent to Beijing Genomics Institute for transcriptional profile analysis.

cDNA synthesis and qRT-PCR

cDNA was synthesized using 0.5 μg yeast total RNA and PrimeScript RT Master Mix according to the manufacturer's protocol. qRT-PCR was performed using SYBR Green Real-time PCR Master Mix on an ABI 7500 Fast Real-time PCR System (ThermoFisher Scientific). cDNA from WT/*Sc*Δ*leuS* cultured in normal medium was used as a control. Data were normalized against the reference gene *ACT1* (53). Primers used for qRT-PCR are listed in Supplementary Table S1.

Protein tags insertion and western blot detection

We inserted the gene sequences encoding 3 × HA tag at the 3' terminus of the *PUT2*, *Pro1*, *Pro3*, *CAR1* and *CAR2* genes, and the sequences encoding 13 × Myc tag at the 3' terminus of the *MCH5* and *PUT1* genes, in both D419A/*Sc*Δ*leuS* and WT/*Sc*Δ*leuS* cells by PCR-mediated homologous recombination (54). Correct integration was confirmed by PCR. After treatment with or without 0.5 mM Nva for 12 h, the yeast cells were harvested and resuspended in ice-cold lysis buffer containing 50 mM Tris–HCl (pH 7.5), 100 mM NaCl, 1 mM EDTA (pH 8.0), 1% Triton X-100, 1 mM PMSF and 1 mM DTT, mixed with a few glass beads, vortexed rigorously for 30 min, then centrifuged at 10 000 × *g* for 15 min, 4°C. The supernatant was collected and proteins were detected by western blot. Anti-HA antibody was obtained from Sigma (H3663), anti-Myc antibody was from Proteintech (66004), anti-beta Actin antibody (ab170325), anti-Hsp70 antibody (ab2787) and anti-Hsp90 antibody (ab13492) were from Abcam.

Detection of Nva misincorporated into proteins

Yeast cells (WT/*Sc*Δ*leuS* and D419A/*Sc*Δ*leuS*) were cultured in 50 ml SD/Leu$^-$ medium for 12 h to A_{600} = 0.6. Each strain was then supplemented with or without 0.5 mM Nva and culturing continued for 12 h. Samples were collected at 2000 × *g* for 5 min, cells were washed twice with 0.9% NaCl, resuspended in buffer B (20 mM HEPES pH 7.5, 140 mM NaCl, 1 mM EDTA pH 8.0, 1% Triton X-100, 10% glycerol, 1 mM DTT, 1 mM PMSF), mixed with a few glass beads, and vortexed rigorously for 1 h. After centrifugation at 12 000 × *g* for 15 min, supernatants were applied to an Amicon Ultra-4 ml centrifugal concentrator (cutoff 3 kDa) and buffer-exchanged three times with buffer C (20 mM HEPES pH 7.5, 140 mM NaCl, 1 mM DTT, 1 mM PMSF) to remove free amino acids. Samples were acid hydrolyzed with 6 M HCl in glass tubes at 95°C for 24 h, and hydrolysates were evaporated to dryness using a rotary evaporator, resuspended in ddH_2O and re-evaporated three times to remove the remaining HCl. Finally, ddH_2O was added to dissolve the remaining residue and centrifuged at 12 000 × *g* for 10 min at 4°C. Supernatants were pretreated using the AccQ-Fluor reagent kit according to the manufacturer's protocol, and samples were analyzed using an AccQ-Tag column (3.9 × 150 mm) (wat052885, Waters) connected to an Alliance separation module (e2695, Waters) and a multi λ fluorescence detector (2475, Waters).

Measurement of intracellular free amino acids

Yeast cells (WT/*Sc*Δ*leuS* and D419A/*Sc*Δ*leuS*) were cultured in SD/Leu$^-$ medium for 12 h to A_{600} = 0.6. Each strain was then supplemented with Nva (0, 0.5, 1 or 2 mM). After 12 h, the A_{600} was measured and samples were collected by centrifugation at 2000 × *g* for 5 min. The collected cells were washed twice with 0.9% NaCl, resuspended in different volumes of ddH_2O according to the amount of yeast cells and boiled at 95°C for 20 min. After centrifugation at 12 000 × *g* for 10 min at 4°C, supernatants were used to measure the intracellular free amino acid content using the same method described above. The amino acids content is expressed as μmol/g yeast (dry weight).

Measurement of cellular ROS

After yeast cells were grown to early exponential phase (A_{600} = 0.6), Nva (0, 0.2, 0.5 or 1 mM) was added to the medium and culturing continued for 4 h. Yeast cells were then collected, washed with 100 mM potassium phosphate buffer (pH = 7.4) and resuspended in 1 ml potassium phosphate buffer. Samples were treated with 58.4 μM 2',7'-dichlorofluorescin diacetate (H_2DCFDA) for 2 h in the dark. After propidium iodide staining, the fluorescence intensity was immediately quantified by flow cytometry using a BD Accuri C6 flow cytometer (BD Biosciences). A minimum of 30 000 yeast cells were analyzed in each sample.

RESULTS

Nva can be efficiently misactivated by *Sc*LeuRS

To explore the editing properties of *Sc*LeuRS, ATP-PPi exchange experiments were initially performed to measure the amino acid activation activity. The results showed that among the non-cognate amino acids, only Nva could be strongly misactivated by *Sc*LeuRS with a discrimination factor of 1/118 (Table 1). This is much higher than the error rate in protein biosynthesis (1/3000) (55), indicating that Nva represents a major threat to the fidelity of *Sc*LeuRS aminoacylation *in vitro*. In contrast, Ile and Val could be well discriminated by *Sc*LeuRS with discrimination factors of 1/11 700 and 1/5900, respectively, both of which are significantly lower than 1/3000 (Table 1).

*Sc*LeuRS-D419A catalyses sufficient Nva-tRNA^{Leu} formation

The high amino acid activation activity of *Sc*LeuRS for Nva suggests that *Sc*LeuRS must possess a robust editing activity to guarantee the accuracy of aminoacylation. The aminoacylation reaction showed that *Sc*LeuRS was barely able to misaminoacylate *Ca*tRNA^{Leu} with Nva and Ile (Table 2). However, in the presence of *Ca*tRNA^{Leu}, the aminoacylation catalytic efficiency of *Sc*LeuRS-D419A, which has lost the post-transfer editing function, for Nva (0.92 $s^{-1}mM^{-1}$) and Ile (0.038 $s^{-1}mM^{-1}$) was 1/67 and 1/1631 of that for the cognate Leu (62 $s^{-1}mM^{-1}$), respectively (Table 2), suggesting that the post-transfer editing pathway plays an important role in preventing Nva and Ile from being mischarged (error rate in protein biosynthesis

Table 1. Amino acid activation kinetics of *Sc*LeuRS with various amino acids

Amino acid	Amino acid structure	K_m (μM)	k_{cat} (s^{-1})	k_{cat}/K_m ($s^{-1}mM^{-1}$)	Discrimination Factor (DF)[b]
Leu	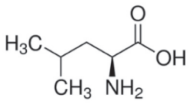	37.6 ± 4.1	102.4 ± 14.7	2723	1
Nva	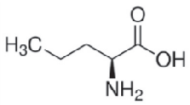	3100 ± 300	71.6 ± 8.0	23.1	1/118
Ile[a]	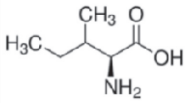	19400 ± 1900	4.5 ± 0.6	0.232	1/11700
Val[a]	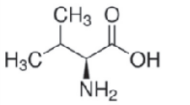	72500 ± 7700	33.7 ± 1.8	0.465	1/5900

The results are presented as the mean ± SD (n = 3).

[a]BioUltra > 99.5%.

[b]DF corresponds to the relative ratio of k_{cat}/K_m for non-cognate amino acids compared with that for Leu.

Table 2. Aminoacylation kinetics of *Sc*LeuRS (WT) and *Sc*LeuRS-D419A (D419A)

Amino acids	*Sc*LeuRS	K_m (μM)	k_{cat}(s^{-1})	k_{cat}/K_m ($s^{-1}mM^{-1}$)	Relative k_{cat}/K_m
Leu	WT	3.3 ± 0.1	0.28 ± 0.04	85	100
	D419A	2.6 ± 0.3	0.16 ± 0.03	62	73
Nva	WT	nd	nd	nd	nd
	D419A	306 ± 28	0.28 ± 0.03	0.92	1.08
Ile[a]	WT	nd	nd	nd	nd
	D419A	1600 ± 100	0.060 ± 0.002	0.038	0.0447
Val[a]	WT	4020 ± 100	0.11 ± 0.02	0.027	0.0318
	D419A	5120 ± 130	0.083 ± 0.017	0.016	0.0188

The results are presented as the mean ± SD ($n = 3$).
[a]BioUltra> 99.5%.
nd, not determined.

is 1/3000) (55). Once the post-transfer editing function of *Sc*LeuRS was disrupted, Nva-$tRNA^{Leu}$ and Ile-$tRNA^{Leu}$ was likely to form (Supplementary Figure S1). Val did not need to be edited because it is only poorly aminoacylated by both *Sc*LeuRS (0.027 $s^{-1}mM^{-1}$) and *Sc*LeuRS-D419A (0.016 $s^{-1}mM^{-1}$; Table 2 and Supplementary Figure S1).

*Sc*LeuRS employs distinguishing post-transfer editing activities for different mischarged products

To further study the post-transfer editing activity of *Sc*LeuRS, deacylation reactions were performed using pre-prepared Nva-*Cat*RNA^{Leu}, Ile-*Cat*RNA^{Leu} and Val-*Cat*RNA^{Leu}. The results showed that *Sc*LeuRS, but not *Sc*LeuRS-D419A, could efficiently deacylate Nva-*Cat*RNA^{Leu} and Ile-*Cat*RNA^{Leu} (Figure 1A–D). In contrast, both *Sc*LeuRS and *Sc*LeuRS-D419A showed minimal deacylation activity for Val-*Cat*RNA^{Leu} (Figure 1E and F). The k_{obs} values for deacylation of Nva-*Cat*RNA^{Leu} and Ile-*Cat*RNA^{Leu} were 0.51 and 0.54 s^{-1}, respectively, which was ∼12-fold higher than that for Val-*Cat*RNA^{Leu} (0.041 s^{-1}; Table 3). These results further suggest that the post-transfer editing function of *Sc*LeuRS is effective for preventing Nva and Ile from attaching to $tRNA^{Leu}$, consistent with a previous report on *Ec*LeuRS (16).

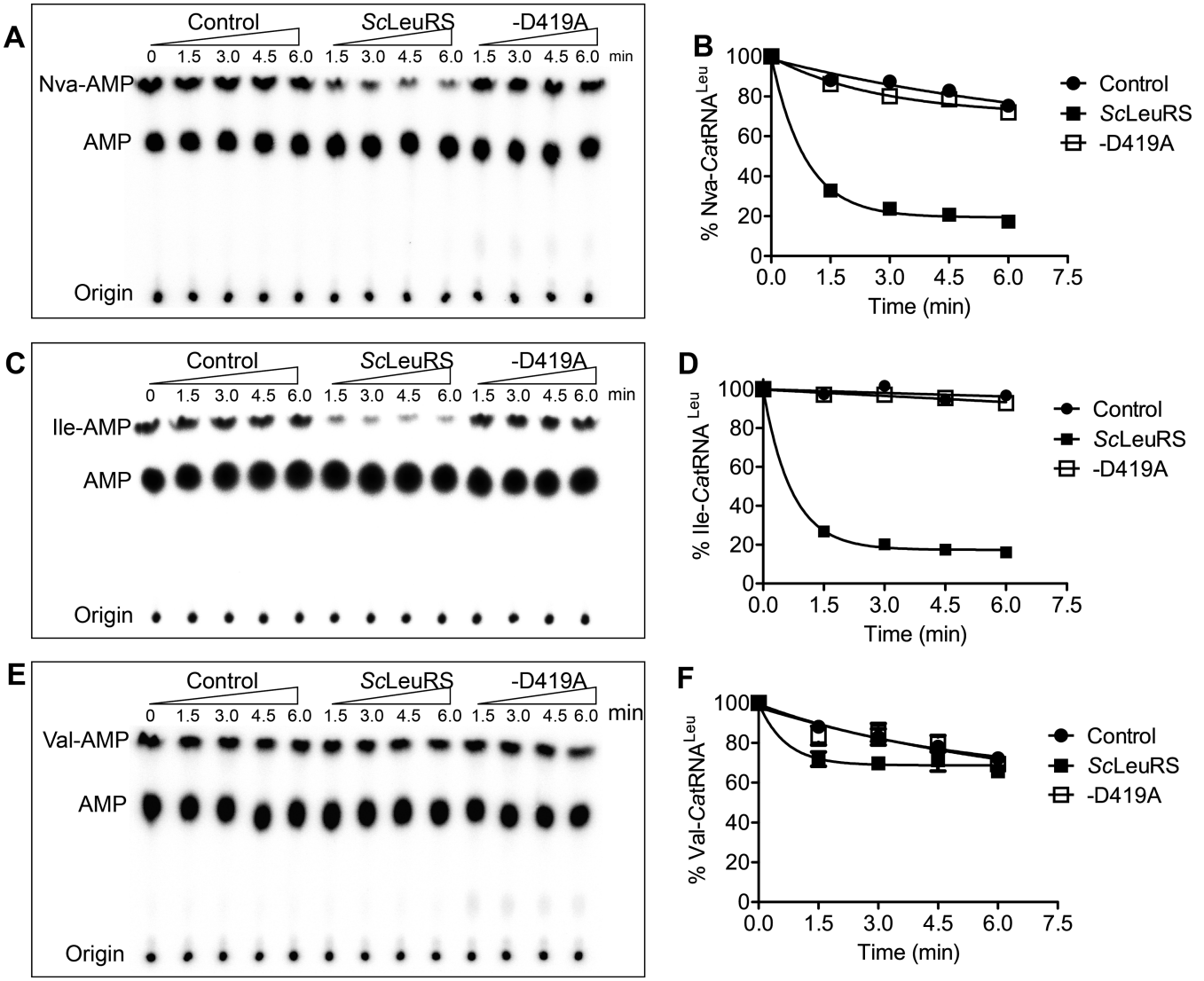

Figure 1. *Sc*LeuRS efficiently deacylates Nva-*Cat*RNA^{Leu} and Ile-*Cat*RNA^{Leu}, but not Val-*Cat*RNA^{Leu}. (**A**, **C** and **E**) Representative images showing the deacylation activities of 100 nM *Sc*LeuRS and *Sc*LeuRS-D419A with 3.5 μM Nva-*Cat*RNA^{Leu} (A), Ile-*Cat*RNA^{Leu} (C) and Val-*Cat*RNA^{Leu} (E) at pH 7.5 based on TLC assays. (**B**, **D** and **F**) Quantification of the deacylation activities of 100 nM *Sc*LeuRS (■) and *Sc*LeuRS-D419A (□) with 3.5 μM Nva-*Cat*RNA^{Leu} (B), Ile-*Cat*RNA^{Leu} (D) and Val-*Cat*RNA^{Leu} (F) in (A), (C) and (E), respectively. Values are the mean ± SD ($n = 3$).

Table 3. Deacylation k_{obs} values for *Sc*LeuRS with misacylated *Cat*RNA^{Leu}

aa-*Cat*RNA^{Leu}	k_{obs} (s^{-1})
Nva-*Cat*RNA^{Leu}	0.51 ± 0.03
Ile-*Cat*RNA^{Leu}	0.54 ± 0.04
Val-*Cat*RNA^{Leu}	0.041 ± 0.004

The results are presented as the mean ± SD ($n = 3$).

Studies on *Ec*LeuRS revealed that the side chain of Thr^{252} limits the size of the 'editing pocket' to prevent the deacylation of the correct product Leu-*Ect*RNA^{Leu} (14,56,57). Given the minimal deacylation activity of *Sc*LeuRS for Val-*Cat*RNA^{Leu}, we postulated that Val might also be excluded by the conserved Thr^{319} (corresponding to Thr^{252} in *Ec*LeuRS) to prevent the hydrolysis of the wrong Val-*Cat*RNA^{Leu} product. Indeed, *Sc*LeuRS-T319A was capable of hydrolyzing both Leu-*Cat*RNA^{Leu} and Val-*Cat*RNA^{Leu}, which verified our hypothesis (Supplementary Figure S2). Therefore, the catalytic site may assume all responsibility for discriminating Val. This distinction in *Sc*LeuRS editing functions might be due to the long-term co-evolution between its aminoacylation and editing activities.

Nva inhibits the growth of D419A/*Sc*Δ*leuS*

Given that Ile and Val could be effectively excluded from the catalytic centre, Nva was deduced to be the biggest threat to the editing function of *Sc*LeuRS *in vitro*. To study the *in vivo* effect of Nva on LeuRS editing-defective yeast, we constructed two strains: WT/*Sc*Δ*leuS* (containing *Sc*LeuRS) and D419A/*Sc*Δ*leuS* (containing *Sc*LeuRS-

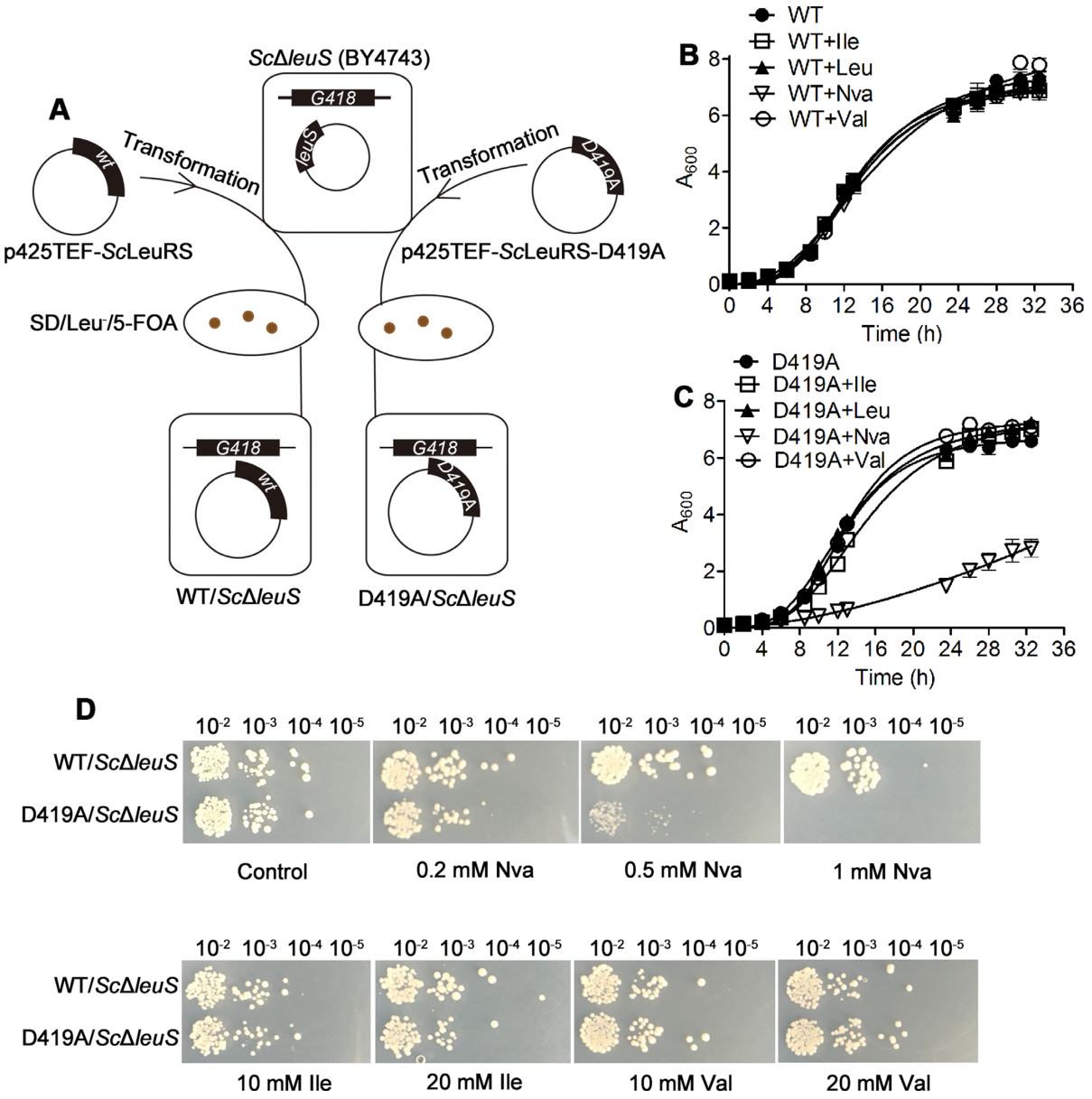

Figure 2. Nva inhibits the growth of LeuRS editing-defective yeast. (**A**) Schematic representation of the construction of yeast strains containing *Sc*LeuRS (WT/*Sc*Δ*leuS*) and *Sc*LeuRS-D419A (D419A/*Sc*Δ*leuS*). (**B** and **C**) Representative growth curves of WT/*Sc*Δ*leuS* (B) and D419A/*Sc*Δ*leuS* (C) in the presence of 0.5 mM Ile (□), Leu (▲), Nva (▽), Val (◯) or the absence of any additional amino acids (●) (initial $A_{600} = 0.1$). Values are the mean ± SD ($n = 3$). (**D**) Growth of yeast cells on SD/Leu$^-$ solid media under various concentration of Nva, Ile or Val.

D419A; Figure 2A). Both yeast strains were cultured in SD/Leu$^-$ medium supplemented with or without 0.5 mM Nva/Ile/Val/Leu (initial $A_{600} = 0.1$). In the absence or presence of various amino acids, WT/*Sc*Δ*leuS* grew at a similar rate (Figure 2B). However, D419A/*Sc*Δ*leuS* grew noticeably slower in the presence of 0.5 mM Nva (Figure 2C). To further confirm the inhibitory effect of Nva on the growth of D419A/*Sc*Δ*leuS*, yeast was spotted on solid SD/Leu$^-$ plates supplemented with varying concentration of Nva (0, 0.2, 0.5 or 1 mM). The growth rate of D419A/*Sc*Δ*leuS* was not affected in the presence of 0.2 mM Nva, but was inhibited more and more obviously with increasing Nva concentration (Figure 2D). This dose-dependent phenotype indicates that Nva is only deleterious for D419A/*Sc*Δ*leuS* cells when its amount exceeds a threshold. In sharp contrast, Ile/Val did not affect the growth of D419A/*Sc*Δ*leuS*, even at a concentration of 20 mM (Figure 2D). This is consistent with the *in vitro* biochemical data that showed Ile and Val were well discriminated by *Sc*LeuRS-D419A. Besides, it should be noted that excess Ile or Val may be used preferentially by their cognate aaRSs to reduce the possibility of misrecognition by *Sc*LeuRS-D419A.

Nva can be misincorporated into the proteome of D419A/*Sc*Δ*leuS*

*Sc*LeuRS-D419A has lost post-transfer editing capac-

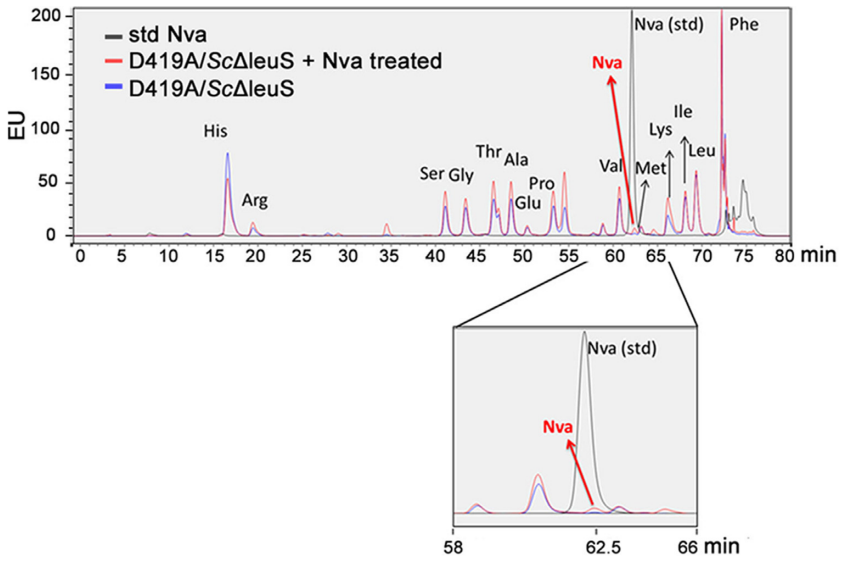

Figure 3. Amino acid composition of the proteome in Nva-untreated and treated D419A/*ScΔleuS*. Black line, standard sample of Nva (0.25 mM); blue line, the constituent amino acids in the proteome of Nva-untreated D419A/*ScΔleuS*; red line, the constituent amino acids in the proteome of Nva-treated D419A/*ScΔleuS*. Amino acids analysis of the proteome of D419A/*ScΔleuS* treated with 0.5 mM Nva revealed a new, small peak eluting after Val at about 62.5 min, corresponding to the Nva standard (std). This peak is absent in that of D419A/*ScΔleuS* without Nva treatment.

ity for Nva, potentially resulting in the accumulation of Nva-tRNA^{Leu} in D419A/*ScΔleuS* under Nva stress conditions. Therefore, we predicted that under such conditions, some Leu residues may be replaced by Nva in the proteome of D419A/*ScΔleuS,* which could jeopardize the translation accuracy. To verify our hypothesis, WT/*ScΔleuS* and D419A/*ScΔleuS* were grown in SD/Leu$^-$ medium supplemented without or with Nva (WT/*ScΔleuS*, WT/*ScΔleuS*+Nva, D419A/*ScΔleuS* and D419A/*ScΔleuS*+Nva). Total proteins were acid hydrolyzed to their constituent amino acids and analyzed by high performance liquid chromatography (HPLC) as described above (see 'Materials and Methods' section). A new, small peak corresponding to the Nva standard was observed in the chromatogram of D419A/*ScΔleuS*+Nva (Figure 3), but not in the chromatograms of D419A/*ScΔleuS* (Figure 3), WT/*ScΔleuS* and WT/*ScΔleuS*+Nva (Supplementary Figure S3). This result further indicates that Nva could be misincorporated into the proteome of D419A/*ScΔleuS* by substituting for some Leu residues.

Heat shock proteins are upregulated in Nva-treated D419A/*ScΔleuS*

Given that Nva is smaller and less hydrophobic than Leu, replacement of Leu by Nva may affect the correct folding of proteins, and the accumulation of misfolded proteins may pose a severe threat to physiological processes and ultimate survival. We therefore proceeded to explore the stress responses in D419A/*ScΔleuS* to Nva stress. By comparing the transcriptional profile of Nva-treated WT/*ScΔleuS* and D419A/*ScΔleuS*, we found that *Hsp70* family proteins *KAR2*, *SSA1* and *SSA2*, and *Hsp90* member *Hsp82* were markedly upregulated in Nva-treated D419A/*ScΔleuS* (Figure 4A), which was further verified by qRT-PCR (Figure 4B–D). The protein level of Hsp70 was significantly upregulated in Nva-treated D419A/*ScΔleuS,* while that of Hsp90 showed slight downregulation (Figure 4E). From this it could be deduced that significant accumulation of misfolded proteins in the cells leads to upregulation of these Hsp70 chaperones to alleviate stress in the Nva-treated D419A/*ScΔleuS* cells, reflecting their ability to facilitate the refolding or degradation of misfolded proteins (35). In contrast, Ile treatment did not induce the upregulation of *Hsp70* and *Hsp90* in D419A/*ScΔleuS*, even at a concentration of 20 mM (data not shown), consistent with its inability to affect cell growth.

Genes related to Pro catabolism are upregulated at the transcription level

Interestingly, most pathways identified by transcriptional profiling were related to cell metabolism (Supplementary Figure S4), suggesting Nva stress may have a global effect on metabolism. In particular, *MCH5*, *PUT1* and *PUT2*, all of which are involved in Pro catabolism, were significantly upregulated in Nva-treated D419A/*ScΔleuS* (Figures 4A and 5A), which was further confirmed by qRT-PCR (Figure 5B–D). However, the expression of these genes was unaffected in Ile-treated D419A/*ScΔleuS* (data not shown), suggesting upregulation of Pro catabolism-related genes may occur in response to Nva misincorporation-induced stress.

We also measured the expression levels of MCH5, PUT1 and PUT2 by the insertion of HA or Myc protein tags (see 'Materials and Methods' section). Unexpectedly, the expression of MCH5, PUT1 and PUT2 were all downregulated in Nva-treated D419A/*ScΔleuS* but not in WT/*ScΔleuS* (Figure 5 E). To interpret the possible reason for the inconsistency between transcriptional and translational levels of these genes, we further measured the expression of other genes, such as the Pro metabolism-related

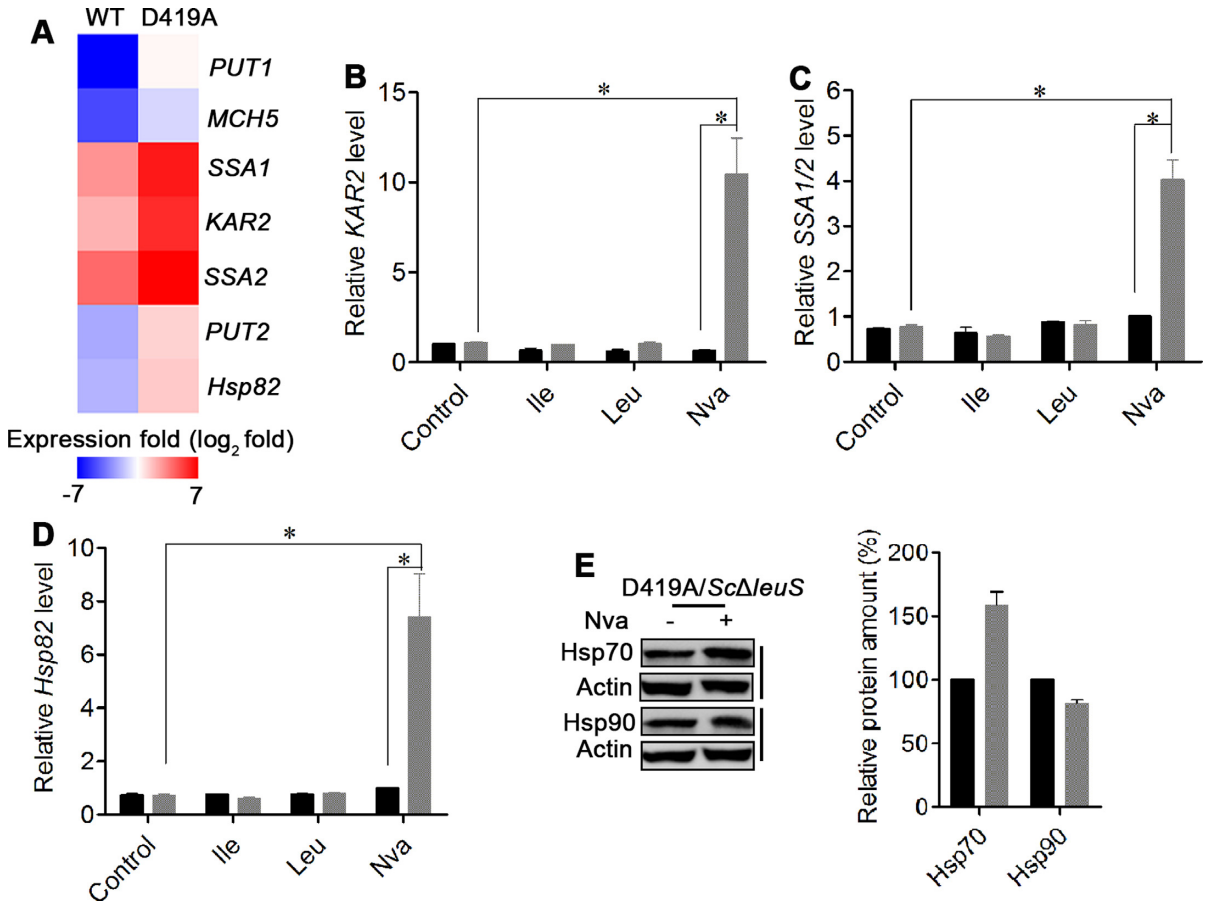

Figure 4. *Hsp70* and *Hsp90* are upregulated in Nva-treated D419A/*ScΔleuS*. (**A**) Transcriptional profile showing genes upregulated (red) or downregulated (blue) over 2-fold in D419A/*ScΔleuS* (D419A) relative to WT/*ScΔleuS* (WT) after treatment with 0.5 mM Nva. (**B**–**D**) qRT-PCR analysis of mRNA levels of *KAR2* (B), *SSA1/2* (C) and *Hsp82* (D) in both WT/*ScΔleuS* (black columns) and D419A/*ScΔleuS* (gray columns) treated with 0.5 mM Ile/Leu/Nva for 12 h (initial $A_{600} = 0.6$). (**E**) D419A/*ScΔleuS* yeast cells were treated with or without 0.5 mM Nva for 12 h (initial $A_{600} = 0.6$). Left panel, protein levels of Hsp70 (70 kDa) and Hsp90 (90 kDa) were determined by immunoblotting. Right panel, quantification of bands in left panel by normalization against Actin. Black columns represent the amount of protein in Nva-untreated D419A/*ScΔleuS*, which is designated as 100%. Gray columns represent the amount of protein in Nva-treated D419A/*ScΔleuS*. Error bars represent the mean ± SD ($n \geq 2$).

proteins (Pro1, Pro3, CAR1 and CAR2), and LeuRS by the insertion of protein tags. The results showed that the expression of these proteins were also downregulated in D419A/*ScΔleuS* after Nva treatment (Supplementary Figure S5). The global decrease in protein amount may result from compromise of translation efficiency under stress and/or the instability of proteins due to Nva misincorporation (58).

Pro, Glu, Gln and Orn accumulate in Nva-treated D419A/*ScΔleuS*

The transcription of *MCH5*, *PUT1* and *PUT2* genes are all activated by Pro utilization trans-activator (PUT3) in the presence of sufficient Pro, suggesting that Pro content may increase in Nva-treated D419A/*ScΔleuS*. It is also of interest to examine the variation of other free amino acids in D419A/*ScΔleuS* after Nva treatment. The data showed that Nva-treated D419A/*ScΔleuS* cells indeed had higher Pro content than Nva-untreated D419A/*ScΔleuS* cells (*t*-test; Figure 6A), indicating the transcription of *MCH5*, *PUT1* and *PUT2* was activated by PUT3 due to the accumulation of Pro. Moreover, Glu, Gln and Orn, all of which are involved in Pro metabolism (Figure 5A), were also found to accumulate in Nva-treated D419A/*ScΔleuS* compared with those in Nva-untreated D419A/*ScΔleuS* cells in a dose-dependent manner (*t*-test; Figure 6B–D and Supplementary Table S2). According to the metabolic pathway, we deduced that there may exist metabolic flow from Orn to Pro and then to Glu and Gln in Nva-treated D419A/*ScΔleuS* cells, leading to the accumulation of Pro, Glu and Gln (Figure 5A). The fact that the medium lacks Pro, Glu and Gln excludes the possibility of their uptake from the medium.

Surprisingly, in the presence of exogenous Nva, less Nva accumulated in the cytoplasm of D419A/*ScΔleuS* than in WT/*ScΔleuS* (*t*-test; Figure 6E), presumably because WT/*ScΔleuS* possesses an editing proficient LeuRS and could tolerate a higher concentration of intracellular Nva. Besides, Nva may be converted to some non-toxic products in D419A/*ScΔleuS* to reduce its cytotoxicity. Given that Nva is an inhibitor of CAR1 and only lacks an amino group compared with Orn (59), it can be deduced that Nva may be converted to Orn or other amino acids in D419A/*ScΔleuS* (Figure 6A), causing the accumulation of Orn.

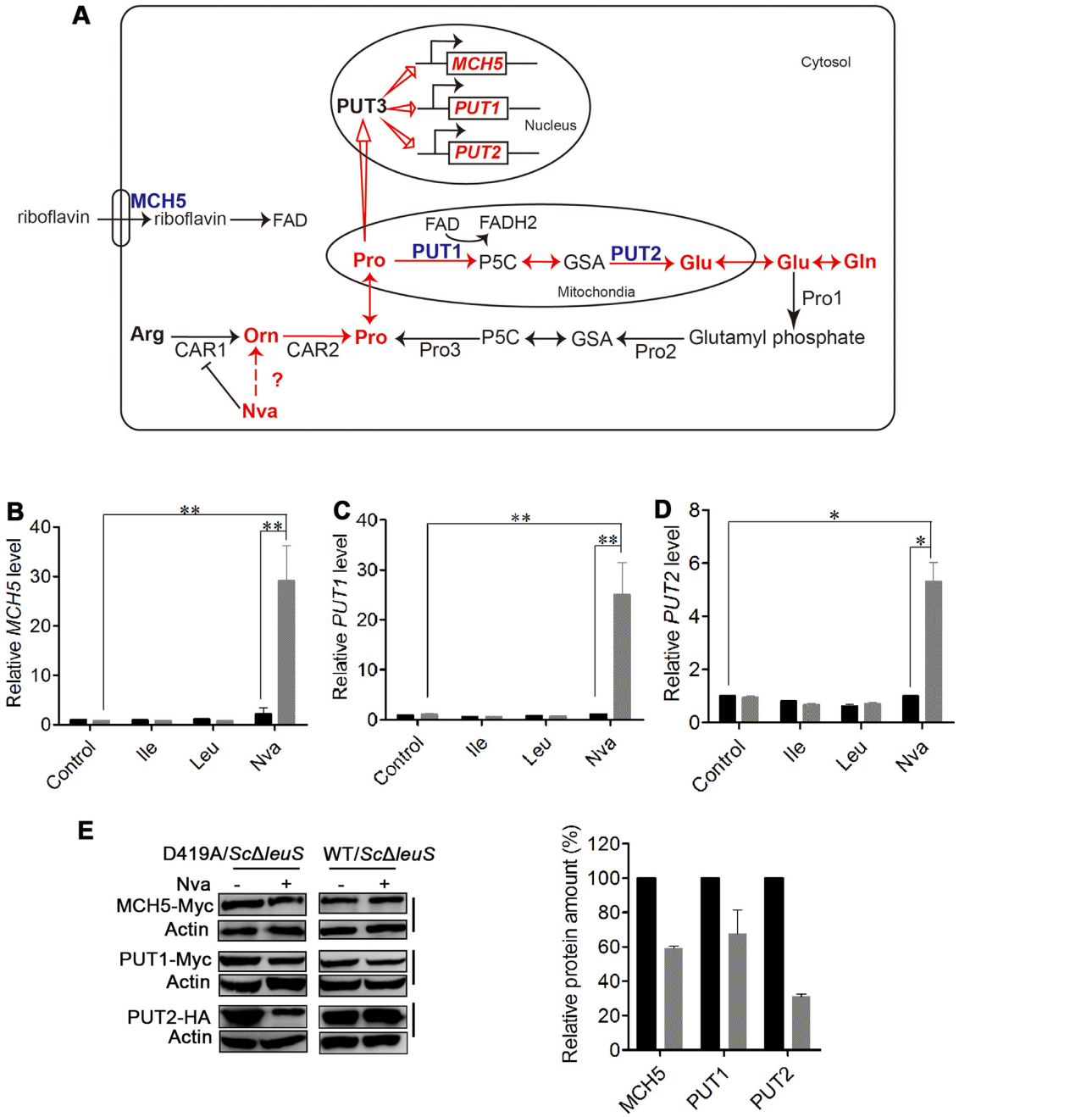

Figure 5. Pro metabolism-related genes are upregulated at the transcriptional level but downregulated at the translational level in Nva-treated D419A/*Sc*Δ*leuS*. (**A**) Schematic overview of Pro metabolism in Nva-treated D419A/*Sc*Δ*leuS*. Amino acids subject to accumulation are shown in red front. Genes subject to over-transcription are shown in red italic front, while proteins subject to downregulation are shown in blue front. Red arrows represent the metabolism direction we suggested, while the red dashed arrow represents the potential conversion. Red hollow arrows represent the regulation of gene transcription. MCH5, riboflavin transporter; PUT1, Pro oxidase; PUT2, P5C dehydrogenase; PUT3, Pro utilization trans-activator. Pro1, γ-glutamyl kinase; Pro2, γ-glutamyl phosphate reductase; Pro3, P5C reductase; CAR1, arginase; CAR2, ornithine aminotransferase. Arg, arginine; Orn, ornithine; Pro, proline; P5C, Δ^1-pyrroline-5-carboxylate; GSA, glutamate-γ-semialdehyde; Glu, glutamic acid; Gln, glutamine; Nva, norvaline. (**B**–**D**) qRT-PCR analysis of mRNA levels of *MCH5* (B), *PUT1* (C) and *PUT2* (D) in WT/*Sc*Δ*leuS* (black columns) and D419A/*Sc*Δ*leuS* (gray columns) treated with 0.5 mM Ile/Leu/Nva for 12 h (initial $A_{600} = 0.6$). Data are normalized against *ACT1* and presented as the mean ± SD ($n = 3$). Asterisks indicate significant differences between different treatments (**$P < 0.02$; *$P < 0.05$; two-tailed Student's *t*-test). (**E**) Both D419A/*Sc*Δ*leuS* and WT/*Sc*Δ*leuS* yeast cells were treated with or without 0.5 mM Nva for 12 h (initial $A_{600} = 0.6$). Left panel, protein levels of MCH5–13 × Myc (90 kDa), PUT1–13 × Myc (85 kDa) and PUT2–3 × HA (70 kDa) were determined by immunoblotting. Right panel, quantification of bands in left panel by normalization against Actin. Black columns represent the amount of protein in Nva-untreated D419A/*Sc*Δ*leuS*, which is designated as 100%. Gray columns represent the amount of protein in Nva-treated D419A/*Sc*Δ*leuS*. Error bars represent the mean ± SD ($n \geq 2$).

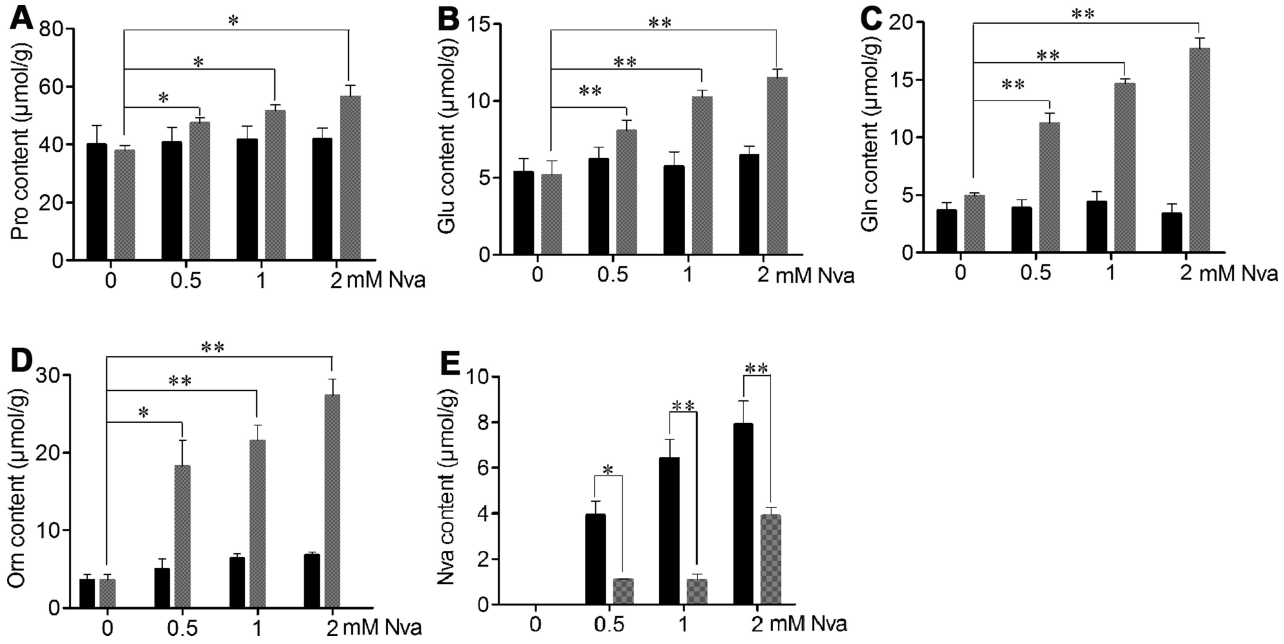

Figure 6. Measurement of free amino acids in Nva-treated D419A/*Sc*Δ*leuS*. (**A**–**E**) Intracellular Pro (A), Glu (B), Gln (C), Orn (D) and Nva (E) content (μmol/g yeast dry weight) of WT/*Sc*Δ*leuS* (black columns) and D419A/*Sc*Δ*leuS* (gray columns) treated with Nva (0, 0.5, 1 or 2 mM) for 12 h (initial $A_{600} = 0.6$). Data are presented as the mean ± SD ($n = 3$). Asterisks represent significant differences between different treatments (**$P < 0.02$; *$P < 0.05$; two-tailed Student's *t*-test).

In contrast, the amount of other amino acids either decreased (Arg, glycine, histidine, lysine and threonine) or showed no obvious change (Ile, Leu, Val, phenylalanine, serine and tryptophan) in Nva-treated D419A/*Sc*Δ*leuS* cells compared with that in Nva-untreated D419A/*Sc*Δ*leuS* cells (*t*-test; Supplementary Table S2), suggesting that Nva stress may affect the metabolism of some other amino acids in LeuRS editing-defective yeast.

Pro, Glu and Gln contribute to lower intracellular ROS levels in Nva-treated D419A/*Sc*Δ*leuS*

As redox homeostasis is indispensable for protein folding (60) and Pro, Glu and Gln are all well documented as antioxidants (37,38,47), we wondered whether the accumulation of these amino acids could decrease ROS levels in Nva-treated D419A/*Sc*Δ*leuS*. WT/*Sc*Δ*leuS* and D419A/*Sc*Δ*leuS* yeast strains were cultured in the absence or presence of Nva, and ROS levels were monitored by flow cytometry using H_2DCFDA as a ROS indicator. As expected, ROS levels in Nva-treated D419A/*Sc*Δ*leuS* were significantly decreased compared with untreated yeast (Figure 7A and B), consistent with the accumulation of Pro, Glu and Gln (Figure 6A–C). In contrast, Nva did not affect ROS levels in WT/*Sc*Δ*leuS* (Figure 7C and D), consistent with the unchanged amount of Pro, Glu and Gln (Figure 6A–C).

To further confirm the important role of intracellular Pro, Glu and Gln in scavenging ROS in Nva-treated D419A/*Sc*Δ*leuS* cells, exogenous Pro, Glu or Gln was added to the medium and ROS levels were monitored. The results showed that the addition of Glu (10 mM), Gln (1 mM) or Pro (10 mM) was enough to lower intracellular ROS levels (Figure 7E and F), further suggesting that accumulation of Pro, Glu and Gln contribute to scavenging of intracellular ROS.

Only Leu, but not Pro, Glu or Gln can strikingly ameliorate Nva stress

As described above, Pro, Glu and Gln accumulated in Nva-treated D419A/*Sc*Δ*leuS* cells, which contribute to lowering ROS levels. In addition to their synthesis *in vivo*, these three amino acids could also be assimilated from the medium. We therefore supplemented Nva-containing minimal medium with these amino acids to identify their function in Nva-treated D419A/*Sc*Δ*leuS*. However, exogenous addition of Pro, Glu or Gln only slightly rescued the Nva-induced growth delay of D419A/*Sc*Δ*leuS* (Figure 8A), indicating that their accumulation may not be a major approach for D419A/*Sc*Δ*leuS* cells to ameliorate Nva stress.

Additionally, Leu was more effective at relieving the Nva-induced growth delay (Figure 8B), presumably by outcompeting Nva. Generally, amino acid analogs enter cells through the same transporter as their corresponding amino acids, but they have a lower affinity for the transporter, resulting in a relatively low transport rate (61). Moreover, cognate amino acids are activated and aminoacylated more efficiently than their analogs, which reduces the possibility of misincorporation when both cognate amino acids and their analogs are present. This is consistent with the observation that an increase in the Leu:Nva ratio decreases Nva misincorporation into haemoglobin (20).

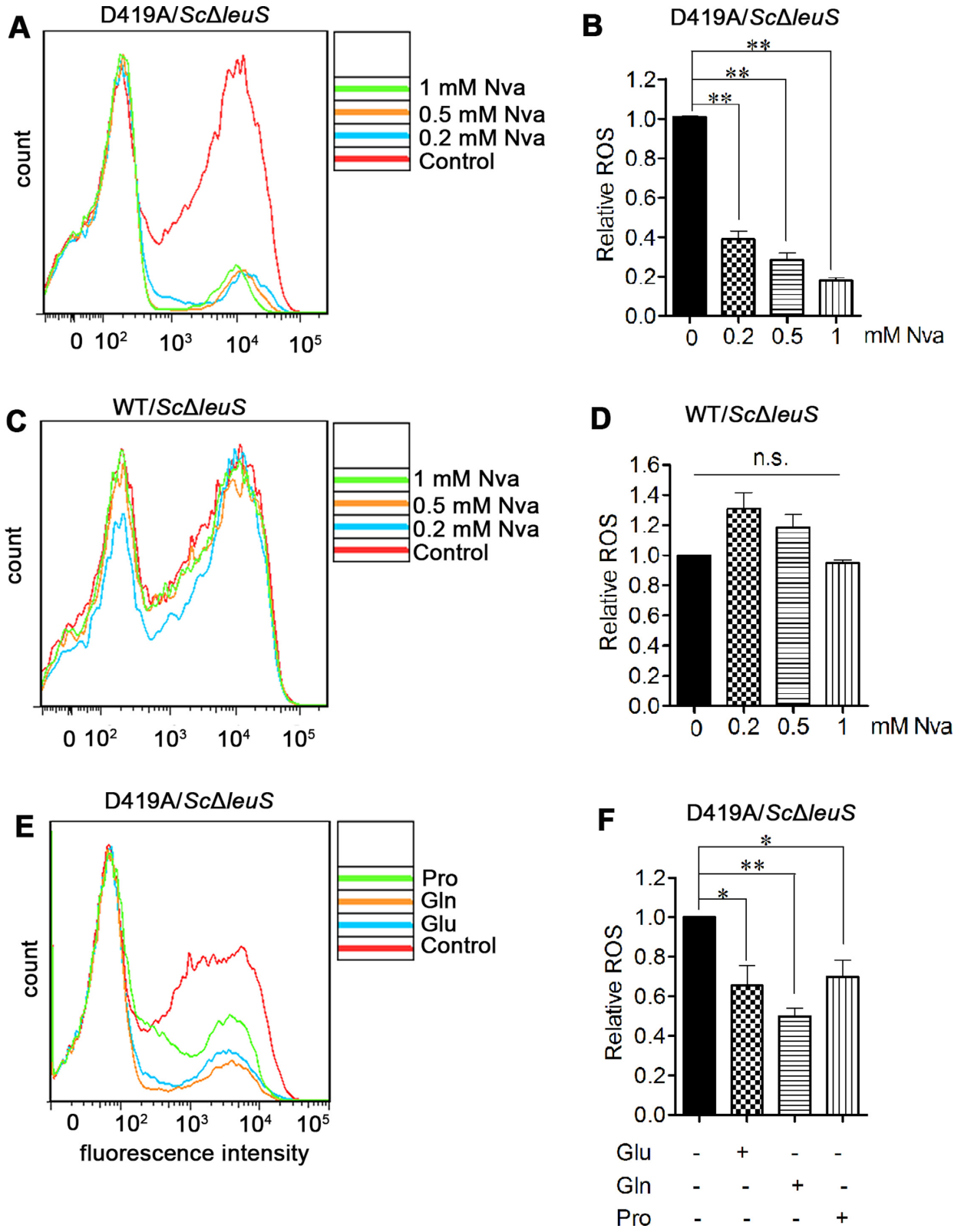

Figure 7. ROS generation in different yeast strains. (**A**) Intracellular ROS levels in D419A/*ScΔleuS* treated with Nva (0, 0.2, 0.5 or 1 mM). Approximately 30 000 cells were counted. Data were processed using Flowjo 2.0 software. The graph shows the ROS intensity in live cells. (**C**) Intracellular ROS levels in WT/*ScΔleuS* treated with Nva (0, 0.2, 0.5 or 1 mM). (**E**) Intracellular ROS levels in D419A/*ScΔleuS* treated with 10 mM Glu, 1 mM Gln and 10 mM Pro. (**B**, **D** and **F**) Quantification of the relative ROS levels in (A, C and E), respectively. Data are the mean ± SD ($n = 3$). *n.s.*, no significant differences between Nva-treated and non-treated WT/*ScΔleuS*. Asterisks indicate significant differences between treated and non-treated D419A/*ScΔleuS* (**$P < 0.02$; *$P < 0.05$; two-tailed Student's *t*-test).

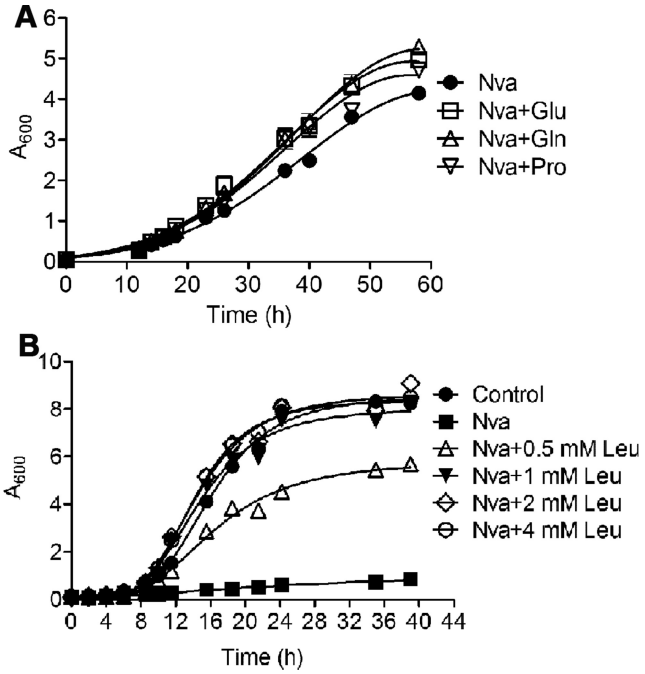

Figure 8. The rescue effects of exogenous Glu/Gln/Pro/Leu on the growth of Nva-treated D419A/*Sc*Δ*leuS* cells. (**A**) Growth curves of D419A/*Sc*Δ*leuS* in the presence of 0.5 mM Nva (●), 0.5 mM Nva +10 mM Glu (□), 0.5 mM Nva +10 mM Gln (△), 0.5 mM Nva +10 mM Pro (▽) (initial A_{600} = 0.1). Values are the mean ± SD (n = 3). (**B**) Growth curves of D419A/*Sc*Δ*leuS* in the presence of 0.5 mM Nva (■), 0.5 mM Nva +0.5 mM Leu (△), 0.5 mM Nva +1 mM Leu (▼), 0.5 mM Nva +2 mM Leu (◇), 0.5 mM Nva +4 mM Leu (○), Control (●) (initial A_{600} = 0.05).

DISCUSSION

Nva is the biggest threat for LeuRS among Leu analogs

Translation is a highly complex process with multiple checkpoints that cooperate to ensure fidelity. AaRSs are key players in this process and their 'double-sieve' mechanism prevents misincorporation of non-cognate amino acids into growing polypeptide chains. Previously, both Nva and Ile were thought to be targets for LeuRS editing. However, it was recently shown that the editing function of *Ec*LeuRS is only required to prevent Nva misincorporation, not misincorporation of Ile (16). Nva is a by-product of Leu metabolism and can accumulate in *E. coli* cells under anaerobic conditions (17). Nva can replace about 10% of Leu residues in the proteome of LeuRS editing-defective *E. coli*, resulting in reduced cell viability (16,18). In the present study, we used the simple eukaryote, *S. cerevisiae*, to reveal that Nva is also the sole threat for eukaryotic LeuRS both *in vitro* and *in vivo*. Once the post-transfer editing function of *Sc*LeuRS was disrupted, some Nva could be misincorporated into the proteome of yeast. Therefore, Nva should be the biggest threat for both prokaryotic and eukaryotic LeuRSs among the various Leu analogs.

Editing deficiency of aaRS inhibits cell growth and could induce diseases

Non-cognate amino acids will be misincorporated into proteins when the editing function of one specific aaRS is deficient, impairing the overall translation fidelity and inducing protein misfolding. Misfolded proteins are extremely deleterious to cells, which may be due to their dysfunction or even toxic gain-of-function. Besides, misfolded proteins are prone to nucleate other proteins to form harmful aggregates. Many studies have shown that the editing deficiency of aaRS can impact many physiological functions including growth (16), neurodegeneration (31), SOS response (33) and apoptosis (34). However, the severity of the cellular responses appears to correlate with the degree of mistranslation. For example, in our study, D419A/*Sc*Δ*leuS* cells could withstand low concentration (0.2 mM), but not higher concentrations (0.5 and 1 mM) of Nva, suggesting that disease or growth inhibition will only occur when the level of misfolded proteins exceed a threshold.

Heat shock proteins are upregulated to deal with misfolded proteins

Proteins must be correctly folded in order to carry out their biological function, thus all cells possess an extensive proteostasis network to cope with misfolded proteins. The upregulation of heat shock proteins by the cell facilitates the refolding or degradation of misfolded proteins, and prevents protein aggregation (35). Indeed, Hsp70 chaperones were upregulated in Nva-treated D419A/*Sc*Δ*leuS*, suggesting the accumulation of misfolded proteins in editing-deficient cells. In particular, the level of the ER chaperone KAR2 (Bip) was strikingly upregulated. KAR2 is also upregulated in AlaRS editing-defective Purkinje cells (31). The ER is an important organelle for protein folding and quality surveillance. The accumulation of misfolded proteins within the ER could disrupt the balance between the unfolded protein load and the ER protein surveillance system, which is known as ER stress. Cells may initiate the unfolded protein responses to relieve ER stress (60).

A new protective response to decreased editing

The lower level of Nva in Nva-treated D419A/*Sc*Δ*leuS* cells compared with that in Nva-treated WT/*Sc*Δ*leuS* cells suggests that Nva may be excluded from the cells or converted into other metabolites, such as α-ketovaleric acid, which could be further converted to other amino acids (17,62). Due to a difference of only an amino group, we assumed that a portion of intracellular Nva may be converted into Orn in Nva-treated D419A/*Sc*Δ*leuS* and Orn could be further converted into Pro, Glu and Gln. By converting Nva into other non-toxic amino acids, cells could reduce the toxicity of Nva.

Pro, Glu and Gln were indeed found to accumulate in Nva-treated D419A/*Sc*Δ*leuS*. Previous studies demonstrated that Pro is a multifunctional molecule (37–39). It can inhibit protein aggregation through interactions with misfolded proteins via the hydrophobic backbone and side-chain (39). Given that misfolded proteins accumulate in

Nva-treated D419A/*Sc*Δ*leuS* cells, the concomitant accumulation of Pro may help prevent protein aggregation. It is noteworthy that, Pro, Glu and Gln are all *bona fide* antioxidants (37,38,47). In our study, we found that both the endogenous accumulation and exogenous addition of Pro, Glu and Gln contributed to lowering ROS generation. Although Pro, Glu and Gln have been studied previously as individual antioxidants, their synergistic action and metabolic modulation in reducing ROS levels has not been described before. However, the exogenous supplementation of Pro, Glu or Gln only slightly relieves the Nva-induced growth inhibition, suggesting that accumulation of antioxidant amino acids (Pro, Glu and Gln) and reduction of ROS may not be major approaches for D419A/*Sc*Δ*leuS* cells to relieve Nva stress but are the products of the metabolic detoxification process.

In conclusion, we explored the intracellular protective mechanism in a LeuRS post-transfer editing-deficient *S. cerevisiae* strain and identified a novel protective pathway to deal with non-cognate amino acids in editing-deficient cells. We propose that the non-cognate amino acid itself has the potential to participate in the protective pathway to reduce its cytotoxicity by conversion to non-toxic amino acids. Our results provide insights into the protective responses in aaRS editing-deficient cells and may assist the development of therapies for editing-deficient diseases.

SUPPLEMENTARY DATA

Supplementary Data are available at NAR Online.

ACKNOWLEDGEMENTS

We are grateful to Prof. Hui-Yong Yin and Mr. Ming-Jiang Zhu (Shanghai Institute for Nutritional Sciences) for their technical assistance in amino acids content measurement. We thank Prof. Jin-Qiu Zhou and Mr. Ming-Hong He (Shanghai Institute of Biochemistry and Cell Biology) for helping us construct the yeast knockout strain. We also thank Prof. Sarah Perrett (Institute of Biophysics, Chinese Academy of Sciences) for her valuable suggestions.

FUNDING

Strategic Priority Research Program of the Chinese Academy of Sciences [XDB19000000]; National Natural Science Foundation of China [31130064, 91440204]. Funding for open access charge: Chinese Academy of Sciences [XDB19000000]; National Natural Science Foundation of China [31130064, 91440204].
Conflict of interest statement. None declared.

REFERENCES

1. Ibba,M. and Söll,D. (2000) Aminoacyl-tRNA synthesis. *Annu. Rev. Biochem.*, **69**, 617–650.
2. Zhou,X.L. and Wang,E.D. (2013) Transfer RNA: a dancer between charging and mis-charging for protein biosynthesis. *Sci. China Life Sci.*, **56**, 921−932.
3. Nureki,O., Vassylyev,D.G., Tateno,M., Shimada,A., Nakama,T., Fukai,S., Konno,M., Hendrickson,T.L., Schimmel,P. and Yokoyama,S. (1998) Enzyme structure with two catalytic sites for double-sieve selection of substrate. *Science*, **280**, 578–582.
4. Fersht,A.R. (1981) Enzymic editing mechanisms and the genetic code. *Proc. R. Soc. Lond. B. Biol. Sci.*, **212**, 351–379.
5. Ling,J., Reynolds,N. and Ibba,M. (2009) Aminoacyl-tRNA synthesis and translational quality control. *Annu. Rev. Microbiol.*, **63**, 61–78.
6. Eriani,G., Delarue,M., Poch,O., Gangloff,J. and Moras,D. (1990) Partition of tRNA synthetases into two classes based on mutually exclusive sets of sequence motifs. *Nature*, **347**, 203–206.
7. Cusack,S., Berthet-Colominas,C., Hartlein,M., Nassar,N. and Leberman,R. (1990) A second class of synthetase structure revealed by X-ray analysis of *Escherichia coli* seryl-tRNA synthetase at 2.5 Å. *Nature*, **347**, 249–255.
8. Burbaum,J.J. and Schimmel,P. (1991) Structural relationships and the classification of aminoacyl-tRNA synthetases. *J. Biol. Chem.*, **266**, 16965–16968.
9. Cusack,S., Yaremchuk,A. and Tukalo,M. (2000) The 2 Å crystal structure of leucyl-tRNA synthetase and its complex with a leucyl-adenylate analogue. *EMBO J.*, **19**, 2351–2361.
10. Silvian,L.F., Wang,J. and Steitz,T.A. (1999) Insights into editing from an Ile-tRNA synthetase structure with $tRNA^{Ile}$ and mupirocin. *Science*, **285**, 1074–1077.
11. Fukai,S., Nureki,O., Sekine,S., Shimada,A., Tao,J., Vassylyev,D.G. and Yokoyama,S. (2000) Structural basis for double-sieve discrimination of L-valine from L-isoleucine and L-threonine by the complex of tRNA(Val) and valyl-tRNA synthetase. *Cell*, **103**, 793–803.
12. Chen,J.F., Guo,N.N., Li,T., Wang,E.D. and Wang,Y.L. (2000) CP1 domain in *Escherichia coli* leucyl-tRNA synthetase is crucial for its editing function. *Biochemistry*, **39**, 6726–6731.
13. Martinis,S.A. and Fox,G.E. (1997) Non-standard amino acid recognition by *Escherichia coli* leucyl-tRNA synthetase. *Nucleic Acids Symp. Ser.*, **36**, 125–128.
14. Tang,Y. and Tirrell,D.A. (2002) Attenuation of the editing activity of the *Escherichia coli* leucyl-tRNA synthetase allows incorporation of novel amino acids into proteins *in vivo*. *Biochemistry*, **41**, 10635–10645.
15. Cvetesic,N., Perona,J.J. and Gruic-Sovulj,I. (2012) Kinetic partitioning between synthetic and editing pathways in class I aminoacyl-tRNA synthetases occurs at both pre-transfer and post-transfer hydrolytic steps. *J. Biol. Chem.*, **287**, 25381–25394.
16. Cvetesic,N., Palencia,A., Halasz,I., Cusack,S. and Gruic-Sovulj,I. (2014) The physiological target for LeuRS translational quality control is norvaline. *EMBO J.*, **33**, 1639–1653.
17. Soini,J., Falschlehner,C., Liedert,C., Bernhardt,J., Vuoristo,J. and Neubauer,P. (2008) Norvaline is accumulated after a down-shift of oxygen in *Escherichia coli* W3110. *Microb. Cell Fact.*, **7**, 30–44.
18. Cvetesic,N., Semanjski,M., Soufi,B., Krug,K., Gruic-Sovulj,I. and Macek,B. (2016) Proteome-wide measurement of non-canonical bacterial mistranslation by quantitative mass spectrometry of protein modifications. *Sci. Rep.*, **6**, 28631–28645.
19. Nandi,P. and Sen,G.P. (1953) An antifungal substance from a strain of *B. subtilis*. *Nature*, **172**, 871–872.
20. Apostol,I., Levine,J., Lippincott,J., Leach,J., Hess,E., Glascock,C.B., Weickert,M.J. and Blackmore,R. (1997) Incorporation of norvaline at leucine positions in recombinant human hemoglobin expressed in *Escherichia coli*. *J. Biol. Chem.*, **272**, 28980–28988.
21. Dulic,M., Cvetesic,N., Perona,J.J. and Gruic-Sovulj,I. (2010) Partitioning of tRNA-dependent editing between pre- and post-transfer pathways in class I aminoacyl-tRNA synthetases. *J. Biol. Chem.*, **285**, 23799–23809.
22. Lincecum,T.L. Jr, Tukalo,M., Yaremchuk,A., Mursinna,R.S., Williams,A.M., Sproat,B.S., Van Den Eynde,W., Link,A., Van Calenbergh,S., Grotli,M. *et al.* (2003) Structural and mechanistic basis of pre- and posttransfer editing by leucyl-tRNA synthetase. *Mol. Cell*, **11**, 951–963.
23. Englisch,S., Englisch,U., von der Haar,F. and Cramer,F. (1986) The proofreading of hydroxy analogues of leucine and isoleucine by leucyl-tRNA synthetases from *E. coli* and yeast. *Nucleic Acids Res.*, **14**, 7529–7539.
24. Tan,M., Zhu,B., Zhou,X.L., He,R., Chen,X., Eriani,G. and Wang,E.D. (2010) tRNA-dependent pre-transfer editing by prokaryotic leucyl-tRNA synthetase. *J. Biol. Chem.*, **285**, 3235–3244.
25. Yao,P., Zhou,X.L., He,R., Xue,M.Q., Zheng,Y.G., Wang,Y.F. and Wang,E.D. (2008) Unique residues crucial for optimal editing in yeast

cytoplasmic leucyl-tRNA synthetase are revealed by using a novel knockout yeast strain. *J. Biol. Chem.*, **283**, 22591–22600.
26. Tukalo,M., Yaremchuk,A., Fukunaga,R., Yokoyama,S. and Cusack,S. (2005) The crystal structure of leucyl-tRNA synthetase complexed with $tRNA^{Leu}$ in the post-transfer-editing conformation. *Nat. Struct. Mol. Biol.*, **12**, 923–930.
27. Fukunaga,R. and Yokoyama,S. (2005) Aminoacylation complex structures of leucyl-tRNA synthetase and $tRNA^{Leu}$ reveal two modes of discriminator-base recognition. *Nat. Struct. Mol. Biol.*, **12**, 915–922.
28. Palencia,A., Crepin,T., Vu,M.T., Lincecum,T.L. Jr, Martinis,S.A. and Cusack,S. (2012) Structural dynamics of the aminoacylation and proofreading functional cycle of bacterial leucyl-tRNA synthetase. *Nat. Struct. Mol. Biol.*, **19**, 677–684.
29. Fang,Z.P., Wang,M., Ruan,Z.R., Tan,M., Liu,R.J., Zhou,M., Zhou,X.L. and Wang,E.D. (2014) Coexistence of bacterial leucyl-tRNA synthetases with archaeal tRNA binding domains that distinguish $tRNA^{Leu}$ in the archaeal mode. *Nucleic Acids Res.*, **42**, 5109–5124.
30. Chen,X., Ma,J.J., Tan,M., Yao,P., Hu,Q.H., Eriani,G. and Wang,E.D. (2011) Modular pathways for editing non-cognate amino acids by human cytoplasmic leucyl-tRNA synthetase. *Nucleic Acids Res.*, **39**, 235–247.
31. Lee,J.W., Beebe,K., Nangle,L.A., Jang,J., Longo-Guess,C.M., Cook,S.A., Davisson,M.T., Sundberg,J.P., Schimmel,P. and Ackerman,S.L. (2006) Editing-defective tRNA synthetase causes protein misfolding and neurodegeneration. *Nature*, **443**, 50–55.
32. Liu,Y., Satz,J.S., Vo,M.N., Nangle,L.A., Schimmel,P. and Ackerman,S.L. (2014) Deficiencies in tRNA synthetase editing activity cause cardioproteinopathy. *Proc. Natl. Acad. Sci. U.S.A.*, **111**, 17570–17575.
33. Bacher,J.M. and Schimmel,P. (2007) An editing-defective aminoacyl-tRNA synthetase is mutagenic in aging bacteria via the SOS response. *Proc. Natl. Acad. Sci. U.S.A.*, **104**, 1907–1912.
34. Nangle,L.A., Motta,C.M. and Schimmel,P. (2006) Global effects of mistranslation from an editing defect in mammalian cells. *Chem. Biol.*, **13**, 1091–1100.
35. Verghese,J., Abrams,J., Wang,Y. and Morano,K.A. (2012) Biology of the heat shock response and protein chaperones: budding yeast (*Saccharomyces cerevisiae*) as a model system. *Microbiol. Mol. Biol. Rev.*, **76**, 115–158.
36. Wang,J., Pareja,K.A., Kaiser,C.A. and Sevier,C.S. (2014) Redox signaling via the molecular chaperone BiP protects cells against endoplasmic reticulum-derived oxidative stress. *Elife*, **3**, e03496.
37. Takagi,H., Taguchi,J. and Kaino,T. (2016) Proline accumulation protects *Saccharomyces cerevisiae* cells in stationary phase from ethanol stress by reducing reactive oxygen species levels. *Yeast*, **33**, 355–363.
38. Krishnan,N., Dickman,M.B. and Becker,D.F. (2008) Proline modulates the intracellular redox environment and protects mammalian cells against oxidative stress. *Free Radic. Biol. Med.*, **44**, 671–681.
39. Ignatova,Z. and Gierasch,L.M. (2006) Inhibition of protein aggregation in vitro and in vivo by a natural osmoprotectant. *Proc. Natl. Acad. Sci. U.S.A.*, **103**, 13357–13361.
40. Saradhi,P.P., Alia,A.S. and Prasad,K.V. (1995) Proline accumulates in plants exposed to UV radiation and protects them against UV induced peroxidation. *Biochem. Biophys. Res. Commun.*, **209**, 1–5.
41. Liang,X., Dickman,M.B. and Becker,D.F. (2014) Proline biosynthesis is required for endoplasmic reticulum stress tolerance in *Saccharomyces cerevisiae*. *J. Biol. Chem.*, **289**, 27794–27806.
42. Sumrada,R.A. and Cooper,T.G. (1984) Nucleotide sequence of the *Saccharomyces cerevisiae* arginase gene (CAR1) and its transcription under various physiological conditions. *J. Bacteriol.*, **160**, 1078–1087.
43. Degols,G. (1987) Functional analysis of the regulatory region adjacent to the cargB gene of *Saccharomyces cerevisiae*. Nucleotide sequence, gene fusion experiments and cis-dominant regulatory mutation analysis. *Eur. J. Biochem.*, **169**, 193–200.
44. Wang,S.S. and Brandriss,M.C. (1986) Proline utilization in *Saccharomyces cerevisiae*: analysis of the cloned PUT1 gene. *Mol. Cell. Biol.*, **6**, 2638–2645.
45. Brandriss,M.C. (1983) Proline utilization in *Saccharomyces cerevisiae*: analysis of the cloned PUT2 gene. *Mol. Cell. Biol.*, **3**, 1846–1856.
46. Reihl,P. and Stolz,J. (2005) The monocarboxylate transporter homolog Mch5p catalyzes riboflavin (vitamin B2) uptake in *Saccharomyces cerevisiae*. *J. Biol. Chem.*, **280**, 39809–39817.
47. Lo,M., Wang,Y.Z. and Gout,P.W. (2008) The x(c)- cystine/glutamate antiporter: a potential target for therapy of cancer and other diseases. *J. Cell Physiol.*, **215**, 593–602.
48. DeBerardinis,R.J. and Cheng,T. (2010) Q's next: the diverse functions of glutamine in metabolism, cell biology and cancer. *Oncogene*, **29**, 313–324.
49. Zhou,X.L., Fang,Z.P., Ruan,Z.R., Wang,M., Liu,R.J., Tan,M., Anella,F.M. and Wang,E.D. (2013) Aminoacylation and translational quality control strategy employed by leucyl-tRNA synthetase from a human pathogen with genetic code ambiguity. *Nucleic Acids Res.*, **41**, 9825–9838.
50. Huang,Q., Yao,P., Eriani,G. and Wang,E.D. (2012) *In vivo* identification of essential nucleotides in $tRNA^{Leu}$ to its functions by using a constructed yeast tRNALeu knockout strain. *Nucleic Acids Res.*, **40**, 10463–10477.
51. Ji,Q.Q., Fang,Z.P., Ye,Q., Ruan,Z.R., Zhou,X.L. and Wang,E.D. (2016) C-terminal domain of leucyl-tRNA synthetase from pathogenic *Candida albicans* recognizes both $tRNA^{Ser}$ and $tRNA^{Leu}$. *J. Biol. Chem.*, **291**, 3613–3625.
52. Ares,M. (2012) Isolation of total RNA from yeast cell cultures. *Cold Spring Harb. Protoc.*, **2012**, 1082–1086.
53. Boer,V.M., Tai,S.L., Vuralhan,Z., Arifin,Y., Walsh,M.C., Piper,M.D., de Winde,J.H., Pronk,J.T. and Daran,J.M. (2007) Transcriptional responses of *Saccharomyces cerevisiae* to preferred and nonpreferred nitrogen sources in glucose-limited chemostat cultures. *FEMS Yeast Res.*, **7**, 604–620.
54. Longtine,M.S., McKenzie,A. 3rd, Demarini,D.J., Shah,N.G., Wach,A., Brachat,A., Philippsen,P. and Pringle,J.R. (1998) Additional modules for versatile and economical PCR-based gene deletion and modification in *Saccharomyces cerevisiae*. *Yeast*, **14**, 953–961.
55. Loftfield,R.B. and Vanderjagt,D. (1972) The frequency of errors in protein biosynthesis. *Biochem. J.*, **128**, 1353–1356.
56. Xu,M.G., Li,J., Du,X. and Wang,E.D. (2004) Groups on the side chain of T252 in *Escherichia coli* leucyl-tRNA synthetase are important for discrimination of amino acids and cell viability. *Biochem. Biophys. Res. Commun.*, **318**, 11–16.
57. Mursinna,R.S., Lee,K.W., Briggs,J.M. and Martinis,S.A. (2004) Molecular dissection of a critical specificity determinant within the amino acid editing domain of leucyl-tRNA synthetase. *Biochemistry*, **43**, 155–165.
58. Holcik,M. and Sonenberg,N. (2005) Translational control in stress and apoptosis. Nature reviews. *Mol. Cell. Biol.*, **6**, 318–327.
59. Saheki,T., Sato,Y., Takada,S. and Katsunuma,T. (1979) Regulation of urea synthesis in rat liver. Inhibition of urea synthesis by L-norvaline. *J. Biochem.*, **86**, 745–750.
60. Santos,C.X., Tanaka,L.Y., Wosniak,J. and Laurindo,F.R. (2009) Mechanisms and implications of reactive oxygen species generation during the unfolded protein response: roles of endoplasmic reticulum oxidoreductases, mitochondrial electron transport, and NADPH oxidase. *Antioxid. Redox Signal.*, **11**, 2409–2427
61. Rodgers,K.J. and Shiozawa,N. (2008) Misincorporation of amino acid analogues into proteins by biosynthesis. *Int. J. Biochem. Cell Biol.*, **40**, 1452–1466.
62. David,S.K., Yoshiro,T., Mostafa,S.M. and David,M.G. (1955) Metabolism of Δ-norvaline-3-C^{14}. *Arch. Biochem. Biophys.***55**. 546–554.